THE MICROWAVE STUDY OF MONO-DEUTERO, MONO-CHLORO CYCLOPROPANE

Thesis for the Degree of M. S.

MICHIGAN STATE UNIVERSITY

Thomas Krigas

1964

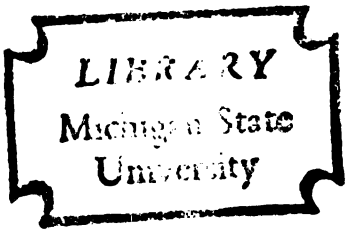

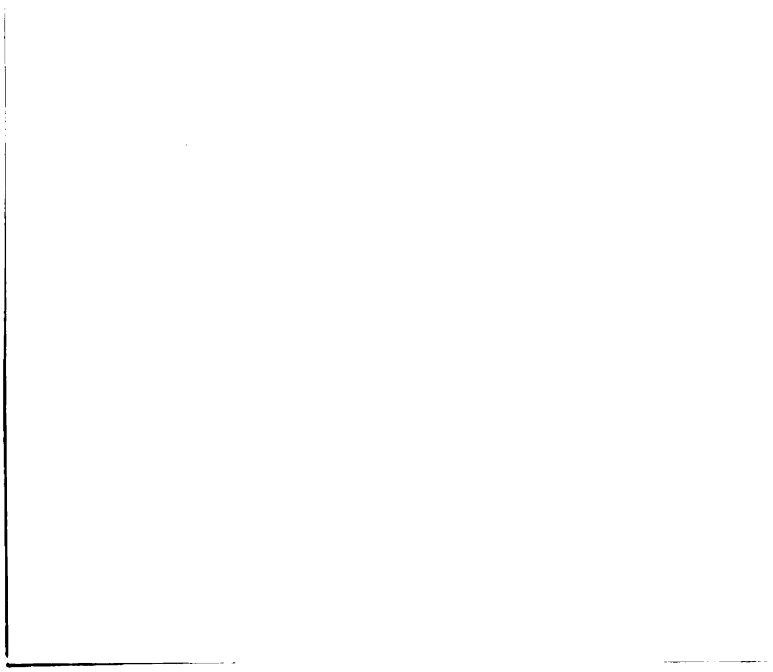

THESIS

ABSTRACT

THE MICROWAVE STUDY OF MONO-DEUTERO,
MONO-CHLORO CYCLOPROPANE

by Thomas Krigas

A short chronological outline of the cyclopropane bonding problem is given. The theoretical aspects of microwave spectroscopy are presented with the emphasis placed on the expressions for the energy levels, selection rules and the perturbations arising from a nuclear quadrupole and/or from an electric field. Also discussed are the calculations, instrumentation and sample preparation.

The pure rotational spectra of the deuterated species $\underline{CHDCH_2CH^{35}Cl}$ (cis), $\underline{CHDCH_2CH^{35}Cl}$(trans), and $\underline{CH_2CH_2CD^{35}Cl}$(sec) have been examined and rotational constants assigned. When these are combined with the remaining four unique isotopic species that have been examined by Dr. G. D. Jacobs and Professor R. H. Schwendeman, a complete substitutional structure is determined. The bond distances and angles are $r(C_1C_2)$ = 1.513 Å, $r(CCl)$ = 1.740 Å, $r(C_2C_3)$ = 1.515 Å, $r(CH)$sec = 1.079 Å, $r(CH)$cis = 1.086 Å, $r(CH)$trans = 1.082 Å, $\angle$ CCCl = 118.7°, $\angle$ ClCH = 115.8° and $\angle$ HCH = 116.2°. If the z principal axis of the quadrupole tensor coincides with the CCl internuclear distance, the quadrupole coupling parameters are χ_{zz} = -71.4 Mc/sec and η bond = 0.029, or χ_{zz} = -73.5 Mc/sec, if a cylindrical charge distribution is assumed. In the light of this structure and its relationship to the structure of similar molecules, the bonding in cyclopropyl chloride is discussed.

THE MICROWAVE STUDY OF MONO-DEUTERO, MONO-CHLORO CYCLOPROPANE

By

Thomas Krigas

A THESIS

Submitted to
Michigan State University
in partial fulfillment of the requirements
for the degree of

MASTER OF SCIENCE

Department of Chemistry

1964

To My Mother and Father

ACKNOWLEDGMENT

I wish to express my appreciation to professor R. H. Schwendeman for his guidance and assistance which he so generously gave during this investigation.

TABLE OF CONTENTS

LIST OF TABLES

LIST OF FIGURES

I. HISTORICAL BACKGROUND

In 1885, Baeyer(1) presented his strain theory to account for the difficulty of small ring formation and for their susceptibility to addition reactions. When his erroneous assumptions of ring planarity for the larger rings (2) and his concept of the inflexible regular tetrahedron (3) were reexamined, a modified theory evolved that was accepted for years.

Since that time, a number of investigators employing heats of combustion (4), specific gravity, melting points, dipole moment (5), electronic spectra (eg. 6,7,8), rates of hydrolysis (9), H-D exchange (10) and dissociation reactions (10,11) have shown pro and con evidence for the existence of resonance energy with transmittance of conjugation in cyclopropane and its derivatives. This anomalous behavior for saturated hydrocarbons has also been treated theoretically (12,13,14). The most complete analysis, that due to Coulson and Moffitt (15), treats the carbon-atom hybridizing ratios as parameters and calculates them by means of the variation technique. Their results for cyclopropane indicate delocalized "bent" bonds with shortened (C-C) distances and the HCH angle = 116°.

In an attempt to resolve some of this small ring controversy and in a continuation of halogenated hydrocarbon studies at Michigan State University, the microwave spectrum of cyclopropyl chloride was examined. Previous structure studies of cyclopropyl chloride with electron diffraction (16) and microwave spectroscopy (17) have been carried out.

The special attraction of microwave spectroscopy stems from two factors: It presents a region of the electromagnetic spectrum previously

inaccessible (0.06 cm^{-1}> wavelength < 30 cm^{-1}) in which many molecules exhibit pure rotational spectra; extremely high resolution is realized when the Hughes-Wilson designed, Stark-modulated instrument is used.

With discarded military radar equipment capable of generating, transmitting, and measuring microwaves, microwave spectroscopy emerged in 1946 as a powerful tool in structure determination. Low pressure gas absorption spectra of NH_3 (18) and OCS (19) in that year not only verified the validity of existing rigid rotor energy solutions but pointed out that hyperfine splittings could arise from Stark effects and nuclear quadrupole moments.

Although both hyperfine splittings greatly complicated the spectra, each afforded additional sources of molecular information. The Stark effect is now commonly used to identify transitions and compute dipole moments. It has been shown by Townes and Dailey (20) that the nuclear quadrupole coupling constants can be related to amounts of ionic and covalent character and hybridization.

To date, the most valuable facet of microwave spectroscopy has been the determination of bond angles and bond distances. In the generally accepted method (21), the differences in the moments of inertia of two isotopically substituted molecules give the coordinates of the substituted atom. Then when all non-equivalent atoms in a molecule have been isotopically substituted a complete structure is obtained.

II. THEORY

2.1 Introduction

The radar development program of World War II produced equipment capable of generating and measuring frequencies in the microwave region of the electromagnetic spectrum from 1 to 1000 kilomegacycles seconds^{-1}. The benefit to molecular spectroscopy was immediately apparent. Here was an experimental method whereby essentially pure rotational transitions of many compounds in their ground electronic and vibrational states could be studied.

Fortunately, the necessary expressions relating these transition energies to molecular parameters had been determined by application of quantum mechanics. The observable frequency is governed by the Bohr condition

$$\nu = \frac{W_2 - W_1}{h} \qquad (2\text{-}1)$$

with W_1 representing the initial and W_2 the final energy state. Energy levels are found as solutions to the equation

$$H\Psi = W\Psi \qquad (2\text{-}2)$$

where H is the quantum mechanical Hamiltonian operator and Ψ is the wave function describing the system. Born and Oppenheimer have shown that the total wave function for a molecule can be separated into an electronic and a nuclear portion. If external forces and nuclear spin are neglected, the nuclear eigenfunction can be expressed as a product of a function for a vibrating non-rotor times a function for a rigid rotor.

Although the case of strong interaction has been worked out, vibrational frequencies are often on the order of 10^4 times those of rotation. For a particular vibrational state, the nuclear position may be considered fixed at the average value over the vibration. The remaining effect, that due to Coriolis coupling, is often ignored.

2.2 Energy Levels

The Hamiltonian for a free rigid rotor in a body-centered corrdinate system becomes

$$H = \frac{\hbar^2}{2}\left[\frac{P_y^2}{I_y}\right] \tag{2-3}$$

$$H = \frac{\hbar^2}{2}\left[\frac{P_x^2 + P_y^2}{I_x}\right] + \frac{\hbar^2}{2}\left[\frac{P_z^2}{I_z}\right] \tag{2-4}$$

$$H = \frac{\hbar^2}{2}\left[\frac{P_x^2}{I_x} + \frac{P_y^2}{I_y} + \frac{P_z^2}{I_z}\right] \tag{2-5}$$

where (2-3) applies to linear, (2-4) to symmetric and (2-5) to asymmetric tops. P_x and I_x are the components of angular momentum and moment of inertia respectively about the x-axis and similarly for the other axes. Rigid rotors are classified as linear if two moments of inertia are equal and the third is zero, as prolate symmetric tops if two moments are equal but greater than the third (cigar shaped), as oblate symmetric tops if two are equal but less than the third (coin shaped), and as asymmetric if all three moments of inertia are different. Obviously, if a unique molecular axis can be distinguished, it has been labeled z. The x, y, z co-ordinates map into the a, b, c co-ordinate designation preferred by spectroscopists, subject only to the proviso $I_c \geq I_b \geq I_a$. (Moments of inertia are discussed in greater detail in Section 2.3).

In a molecule fixed Cartesian co-ordinate system, the matrix elements for angular momenta become

$$(P_y)_{J,K;\ J,K+1} = -i(P_x)_{J,K;\ J,K+1} = \tfrac{1}{2}[J(J+1) - K(K+1)]^{1/2} \quad (2\text{-}6)$$

$$(P_z)_{J,K;\ J,K} = K \quad (2\text{-}7)$$

$$(P_y^2)_{J,K;\ J,K} = (P_x^2)_{J,K;\ J,K} = \tfrac{1}{2}[J(J+1) - K^2] \quad (2\text{-}8)$$

$$(P^2)_{J,K;\ J,K} = P_x^2 + P_y^2 + P_z^2 = J(J+1) \quad (2\text{-}9)$$

The rotational quantum number, J, takes the values J = 0, 1, 2 . . ., while K, the component of angular momentum along a unique molecular axis, becomes K = 0, ±1, ±2, . . . ±J, where $J \geq |K|$. In the preceding matrix elements K may be replaced by M (Section 2.5), where M is the quantum number for the projection of the total angular momentum along a space-fixed axis. In the case where M is substituted for K the sign of i must be changed and x, y, z then refer to space-fixed axes.

The correct energy expressions are obtained by combining the appropriate Hamiltonian equation (2-3) through (2-5) with the angular momentum constraints (2-6) through (2-9). This leads to

$$W_r = \frac{h^2}{8\pi^2 I_b} J(J+1) \quad (2\text{-}10)$$

for linear molecules. For an absorption transition, ΔJ = +1, the Bohr frequency condition (2-1) gives

$$\nu = 2B(J+1) \quad (2\text{-}11)$$

where J is the lower state quantum number and B is called the rotational constant.

$$B \equiv \frac{h}{8\pi^2 I_b} \quad . \tag{2-12}$$

Similar considerations for the symmetric top yield

$$W_r \text{ (prolate)} = h[BJ(J+1) + (A-B)K^2] \tag{2-13}$$

$$W_r \text{ (oblate)} = h[BJ(J+1) + (C-B)K^2] \tag{2-14}$$

with $\nu = 2B(J+1)$ for both cases, since the selection rule requires that $\Delta J = 1$, $\Delta K = 0$ where A and C are also rotational constants defined by

$$A \equiv \frac{h}{8\pi^2 I_a} \quad , \qquad C \equiv \frac{h}{8\pi^2 I_c} \quad .$$

In passing from a symmetric to an asymmetric top, the K double degeneracy is removed, because there is no longer a unique molecular axis. Nevertheless, J remains a "good" quantum number with the total angular momentum P still quantized in units of $h/2\pi\sqrt{J(J+1)}$. There are still $2J+1$ levels for each J. The levels are ordered by a running subscript τ, which takes the values $-J, -J+1, \ldots, +J$. An alternative notation is written as $J_{K_{-1},K_{+1}}$. The number K_{-1} would be the angular momentum about the a-axis in the limiting case of a prolate top, and K_{+1} corresponds to the limiting case of an oblate top with the angular momentum taken about the c-axis. It may be shown that $\tau = K_{-1} - K_{+1}$ and $K_{-1} + K_{+1} = J$ or $J+1$.

Although no closed form solution has been obtained for the energy of an asymmetric top, there are two numerical methods commonly applied. Wang (22) has treated the example of a slightly asymmetric top. For a near-prolate top (B = C), the energy is written as

$$W_r = \left(\frac{B + C}{2}\right) J(J + 1) + \left(A - \frac{B + C}{2}\right) w_\tau^J (b_p) \quad (2\text{-}15)$$

where

$$b_p = \frac{C - B}{2A - B - C} , \quad (2\text{-}16)$$

and

$$w_\tau^J(b_p) = K^2 + C_1 b_p + C_2 b_p^2 \ldots \quad (2\text{-}17)$$

is the reduced energy function. Values of K^2, $C_1 \ldots C_5$ are tabulated for $J \leq 40$ (23). Expressions for a near oblate top ($A \sim B$) can be obtained by replacing b_p with b_0 and interchanging A and C in equations (2-15) through (2-17).

A treatment presented by Ray (24) and extended by King, Hainer and Cross (25) yields the following form for the energy

$$W_r = \left(\frac{A + C}{2}\right) J(J + 1) + \left(\frac{A - C}{2}\right) E_\tau^J(\varkappa) \quad (2\text{-}18)$$

where

$$\varkappa = \frac{2B - A - C}{A - C} , \quad -1 \leq \varkappa \leq 1. \quad (2\text{-}19)$$

Tables of the reduced energy $E(\varkappa)$ from $J = 0$ to $J = 12$ in intervals of 0.01 in $\varkappa$ are given by Townes and Schawlow (26).

The selection rules $\Delta J = 1$, -1 and 0 for asymmetric tops give rise to what are known as the R, P, and Q branches respectively. Individual transitions are also categorized as a, b, or c depending upon the axial component of the dipole moment responsible for the transition. These selection rules are

a type:	ΔK_{-1} = even	ΔK_{+1} = odd,
b type:	ΔK_{-1} = odd	ΔK_{+1} = odd,
c type:	ΔK_{-1} = odd	ΔK_{+1} = even.

2.3 Moments of Inertia and Kraitchman's Equations

The most obvious and useful property of rotational spectra is the ability to calculate a geometrical molecular structure. From a theoretical standpoint one would prefer equilibrium rotational constants (i.e., the values if the atoms were at rest in the lowest molecular potential energy.) Measured values of the rotational constants are related to the equilibrium case by

$$B_{v_1,v_2\ldots} = B_e - \sum_i \alpha_i^B \left(v_i + \frac{d_i}{2}\right) \qquad (2\text{-}20)$$

where $B_{v_1,v_2\ldots}$ is the effective constant, B_e is the equilibrium value of B, the α_i^B's are constants and v_i is the quantum number of ith vibrational mode with d_i the vibrational degeneracy. A structure can be determined for each observed vibrational state, but equation (2-20) demonstrates the difficulty of determining equilibrium values for any but the smallest molecules.

Kraitchman (21) has developed a method whereby the position of an atom in a molecule can be evaluated from the rotational constants of two isotopic species of that atom. His basic assumption states that internuclear distances are unaffected by isotopic substitution. Beginning with the definition of moments of inertia, Kraitchman's argument will be outlined.

The moment of inertia dyadic is defined as (27)

$$I = \sum_i m_i (r_i^2 \vec{1} - \vec{r_i}\vec{r_i}) \; ; \qquad (2\text{-}21)$$

here $\vec{r_i}$ = radius vector from the center of mass to the ith mass

$\vec{1}$ = unit dyadic

m_i = mass of the ith atom.

Typical Cartesian elements are

$$I_{xx} = \sum_i m_i(y_i^2 + z_i^2) , \quad I_{xy} = I_{yx} = -\sum_i m_i x_i y_i ,$$

where I_{xx}, I_{yy} and I_{zz} are called moments of inertia and I_{xy}, I_{xz} and I_{yz} are called products of inertia.

An expedient calculational device is to define a planar dyadic P.

$$P = \sum_i m_i \vec{r_i}\,\vec{r_i} \tag{2-22}$$

with m_i and $\vec{r_i}$ defined as before. This leads to the following typical realtions:

$$I_{xx} = P_{yy} + P_{zz}, \quad P_{xx} = \tfrac{1}{2}(I_{yy} + I_{zz} - I_{xx}), \quad P_{xy} = -I_{xy}. \tag{2-23}$$

According to a theorem of mechanics, there are three mutually perpendicular axes about which the moment of inertia is a maximum or minimum. In this axis system a, b, c, the matrix representations of both dyadics I and P are diagonal with the implicit center of mass conditions

$$\sum_i m_i a_i = 0, \quad \sum_i m_i b_i = 0, \quad \sum_i m_i c_i = 0.$$

Upon isotopic substitution of the s^{th} atom of mass m by $m + \Delta m$, the principal axis of the substituted molecule will in general be translated and rotated from those of the original molecule. The coordinates of the substituted atom in terms of the principal axes of the parent can be expressed with the planar dyadic by making use of the parallel axis theorem. The P matrix becomes

$$P' = \begin{pmatrix} P_{aa} + \mu a_s^2 & \mu a_s b_s & \mu a_s c_s \\ \mu a_s b_s & P_{bb} + \mu b_s^2 & \mu b_s c_s \\ \mu a_s c_s & \mu b_s c_s & P_{cc} + \mu c_s^2 \end{pmatrix} \tag{2-24}$$

where $\mu = \frac{M\Delta m}{M + \Delta m}$, and $M = \sum_i m_i$. Diagonalization of this matrix corresponds to a rotation into the principal axis system of the substituted molecule. Kraitchman has shown that the co-ordinates are

$$| a_s | = \mu^{-1}[(P'_{aa} - P_{aa})(1 + \frac{P'_{bb} - P_{bb}}{P_{bb} - P_{aa}})(1 + \frac{P'_{cc} - P_{cc}}{P_{cc} - P_{aa}})] \qquad (2\text{-}25)$$

Calculation of | b | and | c | is a matter of cyclic permutation of the subscripts.

The sign of a co-ordinate is evaluated from other sources of information, or through chemical intuition. Then when all non-equivalent sites in the molecule have been substituted, each atomic position will be known.

2.4 Nuclear Quadrupole Moments

All nuclei possess an intrinsic spin analogous to that possessed by an electron. The angular momentum I, due to the spinning nucleus, is quantized in units of $h/2\pi$. When $I > 1/2$ a nuclear charge asymmetry results, creating a complex spectrum. This hyperfine splitting is caused by the interaction between the nuclear quadrupole moment and the gradient of the molecular electric field at the nucleus in question. The required orientation restrictions are fulfilled by defining the total molecular angular momentum quantum number F

$$F = J + I, J + I - 1, \ldots |J - I| \qquad (2\text{-}26)$$

such that $F \geq 0$.

Hyperfine splittings are usually small compared to rigid rotor energy level spacings. In this case, the selection rules become $\Delta J = 0, \pm 1$, $\Delta F = 0, \pm 1$, $\Delta I = 0$. The strongest components are produced when $\Delta F = \Delta J$.

Two successful expressions for nuclear quadrupole energy splittings of asymmetric tops have been derived. The first uses the numerically attractive reduced energy function $E^J_\tau(\kappa)$ (28). Here the interaction energy W_Q is

$$W_Q = \frac{1}{J(J+1)} (\chi_{aa} + \chi_{cc})[J(J+1) - \frac{3dE(\kappa)}{d\kappa}] + (\chi_{aa} - \chi_{cc})$$

$$[E(\kappa) - \frac{dE(\kappa)}{d\kappa}] \; Y(F) \qquad (2\text{-}27)$$

where the quadrupole coupling constant χ_{aa} is

$$\chi_{aa} = eQ(\frac{\partial^2 V}{\partial a^2})_{av.}$$

e = electronic charge

Q = electric quadrupole moment,

$(\frac{\partial^2 V}{\partial a^2})_{av.}$ = the average electric field gradient at the $i^{\underline{th}}$ nucleus,

$$Y(F) = \text{Casimir's function} = \frac{3/4\, C(C+1) - I(I+1)J(J+1)}{2(2J-1)I(2I-1)(2J+3)}$$

and $C = F(F+1) - I(I+1) - J(J+1)$.

Casimir's function Y(F) is tabulated from J = 1 to J = 10 for various I and all possible values of F (26,29). The third constant χ_{bb} is found from Laplace's equation. $\chi_{aa} + \chi_{bb} + \chi_{cc} = 0$.

If the molecule is a near symmetric top, then

$$W_Q = \frac{1}{J(J+1)}[(3K^2 - J(J+1) - 3C_2b^2)q_m + (C_1+2C_2b+3C_3b^2)q_m\eta\,]Y(F) \quad (2\text{-}28)$$

where

$$q_m = (\frac{\partial^2 V}{\partial z^2_m})_{av.} = \frac{\chi_{zz}}{eQ}$$

$$\eta = \frac{\partial^2 V/\partial x_m^2 - \partial^2 V/\partial y_m^2}{q_m} = \frac{\chi_{xx} - \chi_{yy}}{\chi_{zz}}$$

with z_m being the molecular principal axis most nearly representing a symmetry axis.

Prior to the spectral analysis, the hyperfine splitting calculations are made on the basis of assumed values of the rotational constants. Once transitions have been assigned and better rotational constants are available, an iterative process of calculation quickly converges both the rotational and quadrupole constants to their experimental values.

Nuclear quadrupole studies are also valuable in explaining the type of bonding between the quadrupolar atom and its adjacent neighbors. The coupling constants obtained from equations (2-27) or (2-28) have their frame of reference in the inertial principal axis system. By means of a similarity transformation, the coupling constant matrix can be rotated into the quadrupole principal axis system. This is accomplished either by assuming that one axis lies along the chemical bond, or by assuming that a cylindrical charge distribution exists about one axis.

Townes and Dailey have shown (30,31) that charge distributions in $\sum_a 1$ molecule arising from adjacent atoms and closed shells of electrons do not contribute appreciably to the quadrupole coupling. Moreover, the amount of ionic character I of a Cl bond is related to the quadrupole coupling constant in the bond direction by

$$I = (1 - s^2 + d^2 + II) - (\chi_{zz}/eQq \text{ atom}) \qquad (2\text{-}29)$$

where s and d are estimates of the amount of hybridization from s and d orbitals, and II is the amount of double bond character.

2.5 Stark Effect

Another complexing spectral factor is introduced when a unidirectional electric field is applied to a molecular system. The energy splittings that occur are known as the Stark effect. This interaction energy between the electric field and the molecular dipole destroys the 2J+1 degeneracy of rotational levels. Components of angular momenta along the space fixed direction of the electric field are quantized in units of $h/2\pi$ and are characterized by M, the magnetic quantum number. M takes the values

$$M = J, J-1 \ldots -J.$$

Stark splittings are often small compared to rotational levels. Therefore, Stark expressions are obtained by standard perturbation calculations. The so-called "first" and "second" order Stark effects indicate the order of perturbation necessary in the calculation. Stark orders also refer to the power of the dipole moment, electric field, and magnetic quantum number which appear in the final equations.

Rotational levels of symmetric tops that exhibit first order Stark will be split into 2J+1 components whereas linear and asymmetric tops which exhibit second order (terms of M^2 only) will be split into J+1 levels. If Stark-modified spectrometers produce fields parallel to the microwave electric field, the selection rule $\Delta M = 0$ holds. As a consequence, the number of Stark components is equal to the lowest J level involved in the transition.

After the assignment has been made, the dipole moment can be evaluated. If the perturbation expansion calculation is made for the asymmetric rotor with the perturbing term μE, the first order energies are zero. The second order splittings from the rigid rotor energy levels are

$$\Delta W_{J,\tau} = E^2 [F^a_{J,\tau} \mu_a^2 + F^b_{J,\tau} \mu_b^2 + F^c_{J,\tau} \mu_c^2] \qquad (2\text{-}30)$$

where μ_a, μ_b, μ_c, are components of the dipole moment in the a, b, c directions; and $F^a_{J,\tau}$ ... are functions of J, τ and M^2 in the a, b, and c directions and can be numerically evaluated.

A Stark component for the transition $J,\tau \longrightarrow J',\tau'$ is due to the difference between two shifted energy levels found from equation (2-30). That is

$$h\nu_{J,\tau;J',\tau'} = E^2[\Delta F^a \mu_a^2 + \Delta F^b \mu_b^2 + \Delta F^c \mu_c^2] \qquad (2\text{-}31)$$

Hence, a plot of frequency of one Stark component versus the value of E^2 for several transitions will afford slopes that allow determination of μ_a, μ_b, and μ_c where the total dipole moment is

$$\mu^2 = \mu_a^2 + \mu_b^2 + \mu_c^2. \qquad (2\text{-}32)$$

III. DESCRIPTION OF THE MICROWAVE SPECTROMETER

A brief description of the microwave spectrometer at Michigan State University will follow the diagram shown in Figure 1. The conventional component outline of a spectrometer into source of energy, absorption cell, detector, and a frequency measuring device will be adopted. For a more complete description, see Jacobs (32) and Tobiason (33).

3.1 Energy Source

The klystron oscillator has a regulated D.C. filament supply used to heat the thermionic cathode. The necessary voltages for the klystron grid, anode and reflector are produced by an FXR type Z815B power supply. The major line voltage fluctuations are eliminated by a Sorensen Model 1000S voltage regulator.

In this laboratory, microwave radiation is generated by reflex klystrons. The electrons emitted by the cathode are accelerated by a positive voltage on the plate and controlled by a grid. Most of the electrons are allowed to pass the plate and enter a deformable cavity. At this point an alternating voltage modulates their velocity forming bunches of electrons. The bunches are repelled by a highly negative electrode at the far end of the tube. Depending upon the cavity size and the phase of the returning electrons, the bunches give up some of their energy to the cavity. Klystrons, available in this laboratory, cover a frequency range from 8 to 37.5 kilomegacycles (kMc).

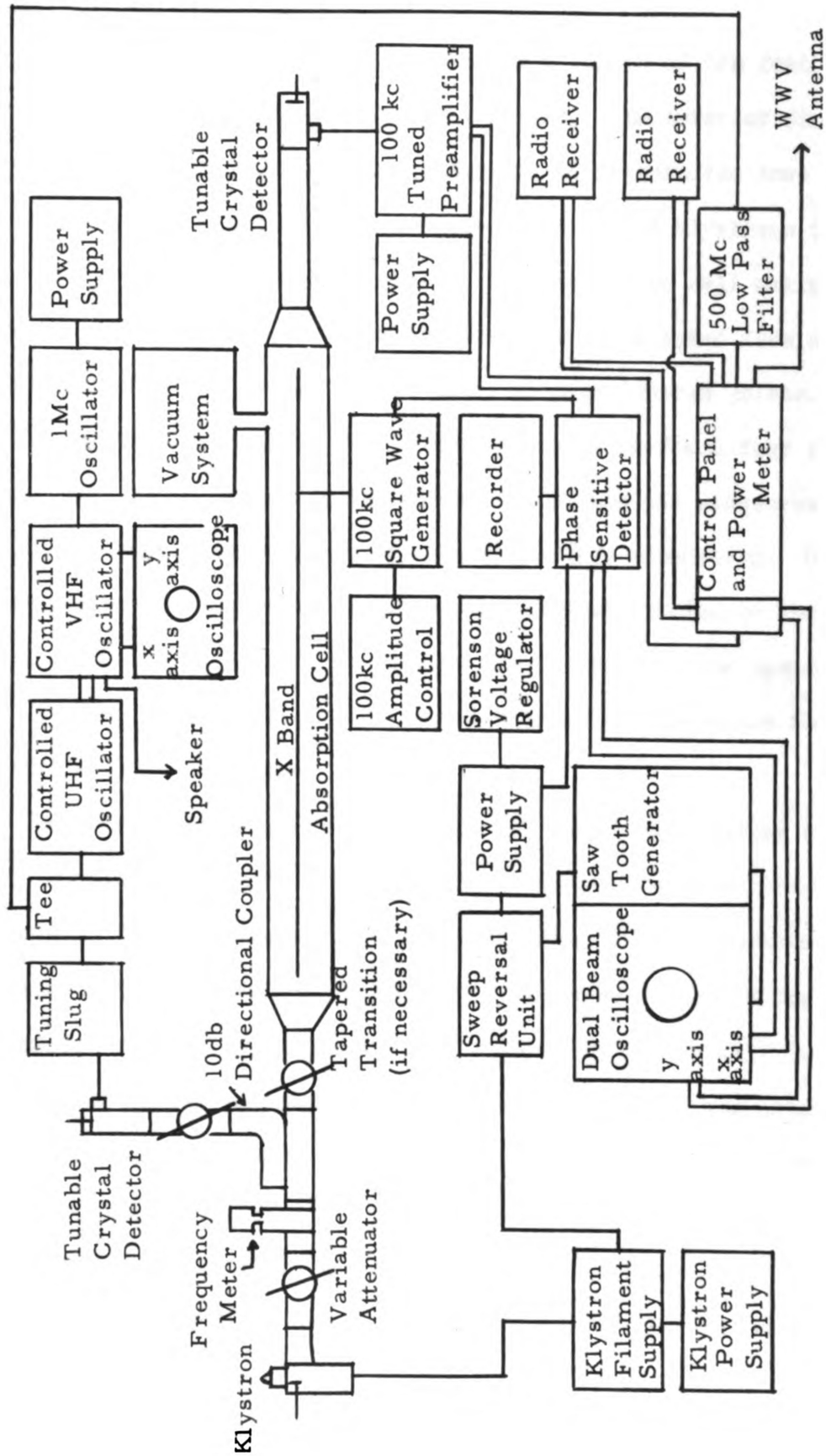

Figure 1. Block Diagram of the Microwave Spectrometer.

3.2 Sample Absorption Cell

The sample cell used in this work has a length of ten feet and is constructed of brass with a silvered interior. The interior dimensions are 0.400" x 0.900" which allows conduction of frequencies down to 8 kMc. Tapered transitions are used to connect K and R-band klystrons to the cell. Mica windows cover both ends of the absorption cell making it a vacuum-tight receptacle. Sample introduction is effected from an external vacuum system sealed to the cells through tapered joints.

In addition to holding the sample, the cell performs four other tasks. Its vacuum-sealed system allows low enough gas pressures (10^{-1} to 10^{-3} mm. Hg) to cancel much of absorption line broadening. Secondly, the sample may be recovered intact by vacuum distillation to the external vacuum line. Third, it permits one to regulate the sample temperature, thereby guaranteeing sufficient energy level population for observing particular transitions.

The fourth task performed is important enough for special consideration. Running the length of the cell is a teflon-insulated silver electrode. This electrode, when coupled with a 100 kc square-wave generator (34), enables one to apply an alternating electric field to the sample. This Stark modulated microwave spectrometer (35) is used to determine dipole moments, identify transitions, and help eliminate instrument noise. The base of the square-wave voltage can be varied to any desired D.C. bias. At a particular D.C. level the amplitude of the voltage has a range from 0 to 1250 volts. Therefore, the sample experiences a periodic field, no-field cycle every 10 microseconds.

3.3 Detection System

Detection is accomplished by silicon crystals that rectify the A.C. output from the absorption cell. The D.C. output from the crystal is sent to an ammeter to indicate the power present at the crystal. Since the microwave voltages of the A.C. output containing the absorption signal are of the order of fractions of microvolts, considerable amplification is necessary. This is accomplished by sending the output through a 100 kc-series resonant combination into a tuned preamplifier-amplifier system. From there, the signal is sent to the phase-sensitive detector which amplified and transmits only those signals in phase and 180^0 out of phase with the 100 kc square-wave reference signal.

The accompanying noise amplification is decreased by the 100 kc tuned load arrangement and numerous filter circuits that reject frequencies differing appreciably from 100 kc. The phase sensitive detector rejects 100 kc noise that is out of phase.

The absorption peaks and Stark components can be displayed in either of two ways. First, the signal from the phase sensitive detector is impressed on the y-axis of an oscilloscope, while the klystron frequency and x-axis of the scope are swept synchronously by a saw-tooth voltage. Thus, one obtains a plot of frequency versus absorption. Second, a recorder can be combined with an automatic klystron drive to permit permanent records to be made.

3.4 Frequency Measurements

Approximate frequency measurements are performed by a cavity-type wavemeter coupled to the waveguide. The size of the cavity is controlled by a micrometer plunger. Oscillations are produced in the wavemeter

when the cavity has the proper dimensions. The small absorption of energy is displayed on the oscilloscope. In this manner, a frequency can be measured within 5 - 20 Mc of the actual value. More accurate measurements are made by measuring the difference frequency between the unknown microwave frequency and a harmonic of a precisely known frequency

$$\nu_{\text{microwave}} = m\,\nu_{\text{standard}} \pm \nu_{\text{difference}}. \qquad (3\text{-}1)$$

The standard frequencies are generated by a Manson Laboratories RD - 140 high-stability one Mc oscillator, a Gertsch Products AM - 1A, V.H.F. interpolator, and a Gertsch FM - 4A microwave frequency multiplier. The generator assembly has an overall precision of 1 part in 10^7 when the oscillator is adjusted by beating its 10th harmonic against the 10 Mc carrier of radio station WWV from the National Bureau of Standards.

The 1Mc RD - 140 oscillator is multiplied 19 to 38 times by the AM - 1A. The output of the multiplier is mixed with the output of a stable 1-2 Mc low-frequency oscillator. The single signal of some frequency between 20 and 40 Mc is input to the FM - 4A. Here, a 500-1000 Mc variable-tuned oscillator is locked to a frequency which is ± 10 Mc from the AM - 1A signal. A crystal diode that is rectifying the microwave signal mixes the standard output of the generator assembly and the microwave signal. Of the many harmonics produced only the difference frequencies less than 500 Mc are sent to the receiver.

The difference frequency is plotted on the y-axis of the second beam of the detection oscilloscope, while the x-axis is the klystron frequency varied with the sawtooth voltage. When this frequency marker is placed directly on the center of the absorption line, the difference frequency can be read directly from the receiver. The two receivers

available in this laboratory are a Collins 30 Mc model 51J4 and a Hallicrafters SX - 62 - A. The overall precision of the frequency measurement process is essentially limited by the receiver. A frequency of 20,000 Mc is precise to 1 part in 10^7 when it is measured by the Collins, while the Hallicrafters is reliable to approximately 1 part in 10^5.

IV. MOLECULAR STRUCTURE OF CYCLOPROPYL CHLORIDE

4.1 Introduction

The investigation of cyclopropyl chloride was prompted by both the small ring "strain" discussions (Section I) and as a continuing study of halogenated hydrocarbons in this laboratory. Once the assignment was completed, the structural parameters and quadrupole constants could be compared with those found in related molecules.

The first partial molecular structure of cyclopropyl chloride was given by O'Gorman and Schomaker (16). Using electron diffraction experiments, they reported

$$r(C\text{-}C) = 1.52 \pm 0.02\text{Å}$$

$$r(C\text{-}Cl) = 1.76 \pm 0.02\text{Å}$$

$$\angle(Cl\text{-}C\text{-ring}) = 56^{\circ} \pm 2^{\circ},$$

where they assumed $r(C\text{-}H) = 1.09\text{Å}$. In 1958, Friend and Dailey (17) studied the Cl - 35 and Cl - 37 species by microwave spectroscopy. They arrived at values for B, C, and the quadrupole coupling constants from the assignment of R-branch, a-type transitions.

Quadrupole coupling constants for the solid assuming cylindrical symmetry have been evaluated from pure quadrupole resonance spectroscopy (36). At 77°K, the reported value is $\chi_{zz} = -68.126$ Mc.

The work of Friend and Dailey was reinvestigated at Michigan State University by Dr. G. D. Jacobs (32). Besides remeasuring the transitions reported earlier, he assigned a series of low J, Q-branch, c-type transitions that are highly sensitive to the A rotational constant. The spectra of the $\underline{CH_2CH_2{}^{13}CH^{35}Cl}$ and $\underline{CH_2{}^{13}CH_2CH^{35}Cl}$ isotopes were

recorded by Professor R. H. Schwendeman while the study of the mono-deutero species are the subject of this thesis.

4.2 Sample Preparation

In the substitution method for structure determination, the molecular parameters of hydrogen atoms can be found by isotopically labeling with deuterium. The equations below represent the synthesis scheme used in preparing the mono-deutero isomers $\underline{CHDCH_2CH^{35}Cl}$(cis), $\underline{CHDCH_2CH^{35}Cl}$(trans), and $CH_2CH_2CD^{35}Cl$(sec). Figure 2 is a projection of cyclopropyl chloride on its a, c plane of symmetry.

$$C_3H_5Cl + 2Li \xrightarrow{\text{ether}} LiCl + C_3H_5Li$$

$$C_3H_5Li + D_2O \xrightarrow{0^oC} C_3H_5D + LiOD$$

$$C_3H_5D + Cl_2 \xrightarrow{h\nu} C_3H_4DCl + C_3H_5Cl + HCl + DCl.$$

The lithium salt, C_3H_5Li was prepared by the method of Hart and Cipriani (37). In this reaction, 7.6 milliliters of distilled cyclopropyl chloride was added over a one hour period to 1.3 grams of lithium in dry diethyl ether at 0^oC. All the apparatus used was flame dried and continuously flushed with argon. At this point, the reaction was allowed to come to room temperature followed by refluxing for one-half hour. The D_2O* was added dropwise to the same reaction vessel now maintained at -78^oC. As the system was slowly warmed, the evolving C_2H_5D gas was collected in a liquid air trap.

From this point on, all steps were performed in the vacuum line. The photochlorination reaction was carried out in a modification of the

*The 99.5% D O was obtained from Liquid Carbonic, 767 Industrial Rd., San Carlos, [2]California.

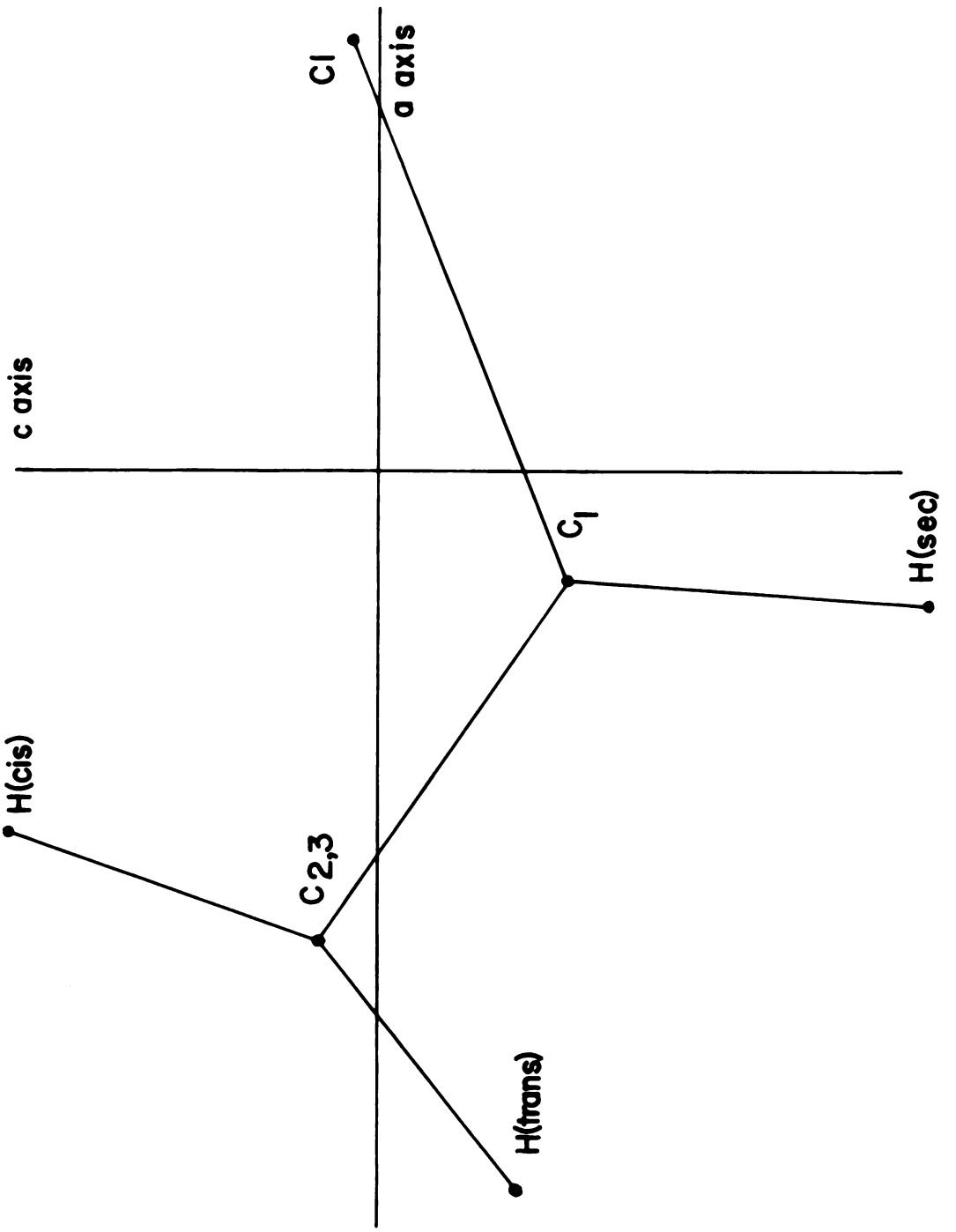

Figure 2. A projection of cyclopropyl chloride in the a,c-plane of symmetry.

method used by Roberts (38) for large scale production of C_2H_5Cl. The light source was a General Electric Ultraviolet Sun Lamp. The C_2H_5D was split into three equimolar samples. Each sample was mixed with chlorine in a two-to-one molar ratio. This mixture was irradiated for two-minute intervals with six to eight passes necessary to react all of the chlorine. Between each pass, chlorinated products were trapped in a bulb cooled by a dry-ice, trichloro ethylene bath (-79°C). The volatile components were removed from the bath by repeated distillation to -196°C. The monochloro product was distilled three times from -10°C to -79°C leaving the polychlorinated material in the bulb cooled to -10°C. The total yield of desired product was 0.68 millimoles or 0.68% of purity greater than 95%. Identification and purity of all compounds were monitored by infrared spectroscopy and gas chromatography.

4.3 Molecular Structure

Before the spectra are examined, an initial calculation is required to obtain approximate values for the principal moments of inertia, energy levels and transition frequencies. A hand calculation was carried out based upon the structure proposed by Friend and Dailey (17).

From the proposed bond distances and angles, the atomic positions can be defined in an arbitrary Cartesian coordinate system (x, y, z). The coordinates of the center of mass (x_m, y_m, z_m) in this axis system are found from the first moment conditions.

$$\sum_i m_i x_i = \sum_i m_i y_i = \sum_i m_i z_i = 0.$$

Translation of the origin to (x_m, y_m, z_m) defines a center of mass coordinate system (x', y', z'), where

$$x' = x - x_m$$
$$y' = y - y_m \qquad (4\text{-}1)$$
$$z' = z - z_m.$$

The eigenvalues of the second moment matrix and therefore the moment of inertia matrix can be computed by a similarity transformation. This operation is equivalent to a rotation of the axes into the principal inertial axis system of the molecule. For cyclopropyl chloride x and y were chosen to lie in the plane of symmetry. As a consequence, z will remain invariant during the transformation and may be identified with the b-axis of Figure 2. Coordinates a_i and c_i are given by

$$a_i = x_i' \cos\theta + y_i' \sin\theta$$
$$c_i = -x_i' \sin\theta + y_i' \cos\theta. \qquad (4\text{-}2)$$

Returning to equation (2-24), the second moments of the substituted molecule may be found by second order perturbation; a typical element is

$$P_{aa'} = P_{aa} + \mu_s a_s^2 + \left[\frac{\mu_s^2 a_s^2 b_s^2}{P_{bb} - P_{aa}}\right] + \left[\frac{\mu_s^2 a_s^2 c_s^2}{P_{cc} - P_{aa}}\right] \qquad (4\text{-}3)$$

where

P_{aa} = the second moment of $\underline{CH_2CH_2CH^{35}Cl}$ in its principal axis system,

$P_{aa'}$ = the second moment of the substituted molecule in its principal axis system,

(a_s, b_s, c_s) = the coordinates of the substituted atom determined from the calculation discussed above.

The moments of inertia are given with respect to their second moments in equation (2-23), while the rotational constants are found by dividing the corresponding moment of inertia into 505, 531 Mc/sec--.a.m.u.-$\mathring{A}^2$.

An independent check on the hand calculation was performed by "MISTIC" the digital computer at Michigan State University. The program written by R. H. Schwendeman is described in detail elsewhere (39).

It should be realized from Figure 2 that the allowed transitions are limited to a and c types, because both the CCl bond and dipole moment lie in the a,c-plane of symmetry. Since the asymmetry parameter, κ, is approximately -0.95 for all three deuterated species, the near prolate top equation (2-15) was applied. When these restrictions are used in conjunction with the Bohr frequency condition (2-1), the R-branch a-type transition frequencies are

$$\nu = 2(J+1)\left[\frac{B+C}{2}\right] + \left[A - \frac{B+C}{2}\right](\Delta K^2 + \Delta C_1 b + \Delta C_2 b^2) \quad (4\text{-}4)$$

while the Q-branch c-type transition $J_{0,J} \longrightarrow J_{1,J}$ frequencies are

$$\nu = \left[A - \frac{B+C}{2}\right](\Delta K^2 + \Delta C_1 b + \Delta C_2 b^2 \ldots). \quad (4\text{-}5)$$

The preliminary calculations indicated a large number of ground vibrational state, R-branch, low J transitions in the 15 to 30 kMc region. A mixture of the deuterated isomers was introduced into the Hughes-Wilson type spectrometer with 100kc Stark modulation (see Section III). An appreciable population density of low J energy levels was maintained by cooling the sample with dry ice. Measurements on stronger transitions were made by oscilloscope display with sweep reversal, while pen-and-ink recordings were employed for the weaker transitions.

The assignment of transitions for $\underline{CHDCH_2CH^{35}Cl}$ (cis and trans) and $\underline{CH_2CH_2CD^{35}Cl}$ were judged on three criteria: one, the transition frequency; two, the quadrupole splittings, multiplicity and intensity; and three, the identification of a duplicate group of v = 0 transitions

arising from the Cl-37 mono-deutero isomers each of which is displaced to a lower frequency from its Cl-35 analogue.

The quadrupole coupling constants fro the deuterated species are nearly the same as those of the parent molecule $\underline{CH_2CH_2CH^{35}Cl}$(32). The hypothetical rigid rotor frequencies are calculated from the experimental multiplets by the following equation

$$\frac{1}{I} \sum_{i} (\nu_i - \nu_{iQ}) = \nu_R \qquad (4\text{-}6)$$

where

ν_i = the experimental transition frequencies

ν_R = the hypothetical unsplit frequency

ν_{iQ} = a function of the quadrupole coupling parameters q_m and $\eta\, q_m$.

Table I is a list of these hypothetical unsplit frequencies.

Although at least ten transitions were assigned for each isomer, the "fit" can usually be considered complete when only two R-branch and two Q-branch transitions give consistent values of A, B and C to within one-tenth of a megacycle. The value of A determined from the $0_{00} \longrightarrow 1_{10}$ transition of $\underline{CH_2CH_2CH^{35}Cl}$ was used to predict Q-branch transition frequencies. This procedure consistently computed values 0.4 megacycles higher than was actually observed. The difference was attributed to centrifugal distortion. Therefore, an empirical factor of 0.4 megacycles was added to all Q-branch transitions before the rotational constants were calculated.

Table II is a comparison of calculated versus observed frequencies for the hyperfine components in trans-deutero cyclopropyl chloride. The rotational constants, moments of inertia and second moments for all isotopic species are given in Table III. Since the requirement of isotopic substitution at every non-equivalent atom has been met, the structure of cyclopropyl chloride can be determined by the method of Kraitchman(Section II-3).

Table I. Hypothetical unsplit frequencies (Mc) for mono-deutero cyclopropyl chloride.

Transition	$CH_2CH_2CD^{35}Cl$	$CHDCH_2CH^{35}Cl$ (cis)	$CHDCH_2CH^{35}Cl$ (trans)
$1_{01} \rightarrow 2_{02}$	14877.49	14770.34	14457.93
$1_{11} \rightarrow 2_{12}$	14676.73	14484.41	14165.55
$1_{10} \rightarrow 2_{11}$	15083.45[a]	15067.26	14761.58
$2_{02} \rightarrow 3_{03}$	22309.35	22141.58	21673.06
$2_{12} \rightarrow 3_{13}$	22013.24	21723.13[a]	21244.88
$2_{11} \rightarrow 3_{12}$		22597.50	22138.86
$3_{03} \rightarrow 4_{04}$	29733.08	29496.47	28871.67
$3_{22} \rightarrow 4_{23}$		29547.12	28922.62[a]
$3_{21} \rightarrow 4_{22}$	29784.89	29602.33	28977.56
$4_{04} \rightarrow 4_{14}$		10111.45	
$5_{05} \rightarrow 5_{15}$	9502.97	9469.53	
$6_{06} \rightarrow 6_{16}$	8906.63[a]	8744.51[a]	9221.25
$7_{07} \rightarrow 7_{17}$	8264.66[a]		8413.19[a]

[a]Uncertainty is ± 0.05 Mc except for frequencies marked "a" for which uncertainty is ± 0.10 Mc.

Table II. Calculated and observed frequencies (Mc) for the hyperfine components in $CHDCH_2CH^{35}Cl$ (trans)

Transition	F - F'	Observed Frequency	Calculated Frequency
$1_{01} - 2_{02}$	5/2 - 7/2	14459.21	14459.16
	3/2 - 5/2		14459.22
	5/2 - 5/2	14444.82	14444.84
$1_{11} - 2_{12}$	5/2 - 7/2	14168.93	14168.82
	3/2 - 5/2	14154.52	14152.54
	5/2 - 5/2	14163.73	14163.84
	3/2 - 3/2	14158.17	14158.10
$1_{10} - 2_{11}$	5/2 - 7/2	14765.28	14765.07
	3/2 - 5/2	14750.95	14750.79
	5/2 - 5/2	14756.13[a]	14755.78
	3/2 - 3/2	14757.46	14757.43
$2_{02} - 3_{03}$	7/2 - 9/2	21673.74	21673.78
	5/2 - 7/2		21673.86
	3/2 - 5/2	21670.18	21670.30
	1/2 - 3/2		21670.21
$2_{11} - 3_{12}$	7/2 - 9/2	22140.30	22140.27
	1/2 - 3/2		22139.63
	5/2 - 7/2	22136.46	22136.72
	3/2 - 5/2		22136.07
$2_{12} - 3_{13}$	7/2 - 9/2	21246.53	21246.31
	1/2 - 3/2		21246.73
	5/2 - 7/2	21242.91	21242.76
	3/2 - 5/2		21243.18
$3_{21} - 4_{22}$	9/2 - 11/2	28872.14	28872.20
	7/2 - 9/2		28872.32
	5/2 - 7/2	28870.35	28870.63
	3/2 - 5/2		28870.52
	7/2 - 7/2	28877.32	28877.23
$3_{22} - 4_{23}$	9/2 - 11/2	28924.90	28924.73
	7/2 - 9/2	28919.00	28919.03
	5/2 - 7/2	28920.70	28921.03
	3/2 - 5/2	28926.78	28926.73

Table II. Continued.

Transition	F - F'	Observed Frequency	Calculated Frequency
$6_{06} - 6_{16}$	15/2 - 15/2	9220.18	9220.18
	13/2 - 13/2	9222.80	9222.92
	11/2 - 11/2	9222.20	9222.27
	9/2 - 9/2	9219.62	9219.54
$7_{07} - 7_{17}$	17/2 - 17/2	8411.95	8412.35
	11/2 - 11/2		8411.88
	15/2 - 15/2	8414.36	8414.69
	13/2 - 13/2		8414.21

[a]Interfering transition.

Table III. Rotational constants (Mc)[a], moments of inertia (a.m.u. - $\AA^2$)[b,c] and second moments (a.m.u. - $\AA^2$), for various species of cyclopropyl chloride.

Species	A	B	C	I_a	I_b	I_c	P_{aa}	P_{bb}	P_{cc}
$CH_2CH_2CH^{35}Cl$[d]	16536.2	3905.44	3622.46	30.5711	129.4428	139.5546	119.2132	20.3415	10.2296
$CH_2CH_2CH^{37}Cl$[d]	16529.2	3810.27	3540.78	30.5841	132.6759	142.7739	122.4328	20.3411	10.2430
$CH_2CH_2{}^{13}CH^{35}Cl$[e]	16368.5	3892.72	3619.74	30.8844	129.8657	139.6595	119.3204	20.3391	10.5453
$^{13}CH_2CH_2CH^{35}Cl$[e]	16224.3	3845.79	3557.75	31.1589	131.4505	142.0929	121.1922	20.9006	10.2582
$CH_2CH_2CD^{35}Cl$[f]	15209.8	3821.69	3618.34	33.2372	132.2794	139.7135	119.3778	20.3356	12.9016
$CHDCH_2CH^{35}Cl$ (cis)[f]	15194.0	3839.64	3548.28	33.2718	131.6610	142.4721	120.4306	22.0414	11.2303
$CHDCH_2CH^{35}Cl$ (trans)[f]	15662.1	3764.84	3466.90	32.2773	134.2769	145.8164	123.9080	21.9084	10.3689

[a]Uncertainty in rotational constants estimated as follows: A, ± 0.4 Mc; B and C, ± 0.03 Mc.

[b]Uncertainty in moments of inertia estimated as follows: A, ± 0.0008 a.m.u. - $\AA^2$; B and C, ± 0.0011 a.m.u. - $\AA^2$.

[c]Conversion factor used = 505,531 Mc - a.m.u. - $\AA^2$.

[d]References (17) and (32).

[e]R. H. Schwendeman, Private communication.

[f]This work.

The resultant coordinates are shown in Table IV where $\underline{CH_2CH_2}CH^{35}Cl$ has been taken as the "parent" molecule.

It will be recalled that Kraitchman's equations are derived for a rigid molecule. However, in a physically real situation, the zero-point vibrations change upon isotopic substitution producing slight deviations from these formulas. With zero-point errors likely to be as high as 1% in the bond distances and angles calculated, the approximations necessary to interpret the data prove the most serious limitation to microwave, especially when one considers that frequency measurements are accurate to about 0.0001%.

Earlier workers often reported structures (called r_0 structures) calculated by adjusting the bond distances and angles to fit the observed moments of inertia of a small number of isotopic substitutions. Costain (40) has compared these r_0 structures to both the substitutional structures obtained from Kraitchman's equations (r_s) and the equilibrium structures (r_e) of simple molecules that have been vibrationally analyzed. He found the r_s structures to be closer to the r_e structures with much smaller mean deviations than is the case of the r_0 method.

This pragmatic justification of the substitution procedure is impaired when heavy atom coordinates are less than 0.15Å from an axis (eg., the c-coordinates of Cl, C_2 and C_3 in cyclopropyl chloride). Fortunately, the c-coordinates of C_2 equals that of C_3. The two independent heavy atom c-coordinates, C_2 or C_3 and Cl, can be corrected for zero-point vibrational effects by applying the two conditions

$$\sum_i m_i c_i = \sum_i m_i a_i c_i = 0.$$

Table IV. Coordinates ($\mathring{A}$) of the atoms in cyclopropyl chloride.

Atom	a	b	c
-Cl	1.2861	0	0.0841
C_1	-0.3287	0	-0.5647
$C_{2,3}$	-1.4093	± 0.7577	0.1760
H (sec)	-0.4022	0	-1.6407
H (cis)	-1.0925	± 1.2493	1.0908
H (trans)	-2.1552	± 1.2765	-0.4109

$$\sum_i m_i a_i = 0.2368 \text{ a.m.u.} - \mathring{A}$$

$$\sum_i m_i c_i = 0.2514 \text{ a.m.u.} - \mathring{A}$$

$$\sum_i m_i a_i c_i = 0.1045 \text{ a.m.u.} - \mathring{A}^2$$

$$I_a = 30.4873 \text{ a.m.u.} - \mathring{A}^2$$

$$I_b = 129.0440 \text{ a.m.u.} - \mathring{A}^2$$

$$I_c = 138.9874 \text{ a.m.u.} - \mathring{A}^2$$

Inserting the new coordinates into Kraitchman's equations yields structure II of Table V. A degree of satisfaction is achieved by noting that within experimental error structure II agrees with Structure I obtained with no correction terms.

Because detailed vibrational analyses of complicated molecules are neither experimentally or theoretically feasible, Laurie (41) has suggested a calculation to estimate the uncertainty of r_s structures. When a site is substituted by a heavier isotope, the coordinates obtained give an apparent average bond shortening which may be as large as 0.0001Å. Although it is difficult to ascribe the vibrational effect to any single effect, for calculational purposes Laurie takes the point of view that when a heavy atom is substituted all the bonds to that atom are actually shortened. Then the second moments and their corresponding coordinates are computed for the following hypothetical molecules: (1) $C_3H_5{}^{35}Cl$ with the parameters in Table V, (2) $C_3H_5{}^{37}Cl$ with the parameters in Table V except r(CCl) shortened by 0.00005Å, (3) $\underline{CH_2CH_2}{}^{13}CH^{35}Cl$ with the parameters in Table V except r(CCl) and both $r(C_1C_2)$ shortened by 0.00005Å, and (4) $^{13}\underline{CH_2CH_2}CH^{35}Cl$ with the parameters in Table V except $r(C_2C_3)$ and the appropriate $r(C_1C_2)$ shortened by 0.00005Å. Table VI contrasts coordinates and parameters of the r_s structure and the one obtained by the bond shortening. Note that the small change estimated upon isotopic substitution results in significant changes in the structural parameters. The greatest change is in the a-coordinate of C_1 where three bonds are involved in the shortening. The large change is due to the large uncertainty inherent in the substitution method when coordinates are less than 0.15Å (see above) as they are in the c-coordinates of C_1, C_2 and C_3.

Table V. Bond distances (Å) and bond angles (degrees) for cyclopropyl chloride.

Parameter	Distance or angle		Uncertainty	
	I_a	II_b	Total	Experimental
CCl	1.740	1.740	+.011 -.003	±.003
$C_1C_{2,3}$	1.513	1.512	+.006 -.008	±.004
C_2C_3	1.515	1.517	+.003 -.001	±.001
CH (sec)	1.079	1.080	±.003	±.001
CH (cis)	1.086	1.086	+.006 -.008	±.004
CH (trans)	1.082	1.079	+.010 -.004	±.003
CCCl	118.7	118.9	+.3 -.6	±.3
ClCH	115.8	115.7	+.3 -.4	±.2
CCH (sec)	116.1	116.0	+.8 -.5	±.3
C_1C_3H (cis)	115.5	115.5	+.6 -.2	±.2
C_2C_3H (cis)	116.9	116.9	+.6 -.6	±.4
C_1C_3H (trans)	117.8	118.1	+.4 -1.0	±.4
C_2C_3H (trans)	118.7	118.7	+.5 -.6	±.3
HCH	116.2	116.0	+.6 -.4	±.3

[a]Structure I is taken directly from Kraitchman's equations.

[b]Structure II is calculated by correcting the coordinates of the heavy atoms so that $\sum_i m_i c_i = 0$ and $\sum_i m_i a_i c_i = 0$, where $\sum_i m_i a_i$ becomes 0.2367 a.m.u. - Å.

Table VI. Comparison of coordinates (Å), bond distances (Å), and bond angles (degrees) of heavy atoms computed from the Kraitchman equations assuming (a) no reduction in bond lengths, and (b) 0.00005 Å reduction in bond lengths.

Parameter	No Reduction	0.00005 Å Reduction
a(Cl)	1.2861	1.2852
c(Cl)	0.0841	0.0837
$a(C_1)$	-0.3287	-0.3184
$c(C_1)$	-0.5647	-0.5644
$a(C_{2,3})$	-1.4093	-1.4091
$b(C_{2,3})$	±0.7577	±0.7567
$c(C_{2,3})$	0.1760	0.1759
r(CCl)	1.740	1.729
$r(C_1C_2)$	1.513	1.520
$r(C_2C_3)$	1.515	1.513
< CCCl	118.7	118.9

A new approach to uncertainty calculations has been proposed by Tobiason and Schwendeman (42). In planar molecules such as H_2O and H_2CO the second moments perpendicular to the molecular plane should be zero. However, the out-of-plane vibrations give rise to a slight deviation called the inertial defect. If the a-axis is perpendicular to the place of the molecule, then

$$P_{aa} = \sum_i m_i a_i^2 = 0 \qquad (4\text{-}7)$$

no longer holds exactly, but

$$2P_{aa}^{e} = (I_{bb} + I_{cc} - I_{aa}) + \Delta_{aa} = 2P_{aa} + \Delta_{aa} \qquad (4\text{-}8)$$

does, where

P_{aa} = the effective second moment about the a-axis

P_{aa}^{e} = the equilibrium second moment about the a-axis

Δ_{aa} = the inertial defect.

If equation (4-8) is placed in Kraitchman's equation (2-25) where in the general case Δ_{aa} is a quasi-inertail defect that retains its significance as a lumped, ground-state vibrational correction term, one gets

$$\left|a^{e}\right| - \left|a\right| = \left|2a\mu\right|^{-1} \left\{ \left[1 + \frac{P_{bb'} - P_{bb}}{P_{bb} - P_{aa}}\right] \left[1 + \frac{P_{cc'} - P_{cc}}{P_{cc} - P_{aa}}\right] \left[\frac{\Delta_{aa'} - \Delta_{aa}}{2}\right] \right. \qquad (4\text{-}9)$$

$$\left. + \left[\frac{1}{2}(P_{aa'} - P_{aa})\right] \left[\left(1 + \frac{P_{cc'} - P_{cc}}{P_{cc} - P_{aa}}\right) \left(\frac{\Delta_{bb'} - \Delta_{bb}}{P_{bb} - P_{aa}}\right) + \left(1 + \frac{P_{bb'} - P_{bb}}{P_{bb} - P_{aa}}\right) \left(\frac{\Delta_{cc'} - \Delta_{cc}}{P_{cc} - P_{aa}}\right) \right] \right\}$$

Terms involving products of changes in the inertial defect have been ignored as have the differences between equilibrium and effective second moments in the denominator of equation (4-9). Such terms are ordinarily smaller than those retained.

If the magnitudes of $(\Delta_{aa'} - \Delta_{aa})$ etc., are roughly equal, the last two terms may be dropped since $\frac{\Delta_{bb'} - \Delta_{bb}}{P_{bb} - P_{aa}}$ and similar quantities are quite small in comparison. The coordinate uncertainties $|a^e| - |a|$ can then be related to bond distances and angles by employing the total differential. If $r_{s,t}$ is the distance between atoms s and t, then

$$r_{s,t} = \underline{fn}\,(a_s, b_s, c_s; a_t, b_t, c_t)$$

and

$$\delta r_{s,t} = \frac{\partial r_{s,t}}{\partial a_s}\delta a_s + \frac{\partial r_{s,t}}{\partial a_t}\delta a_t + \frac{\partial r_{s,t}}{\partial b_s}\delta b_s + \ldots + \frac{\partial r_{s,t}}{\partial c_t}\delta c_t. \quad (4\text{-}10)$$

Of course, angle uncertainties require changes in three atoms.

Table VII contains the values for $|a^e| - |a_s|$ etc., for each atom assuming 0.001 a.m.u. - $\mathring{A}^2$ for $\Delta(\Delta_{aa})$. Laurie indicated that the vibrational contribution to the coordinate is positive while the experimental uncertainty can have either sign. The experimental portion was calculated using an estimated 0.002 a.m.u. - $\mathring{A}^2$ change in the inertial defect. Both the experimental and total uncertainties in the structural parameters are listed in Table V, where the total uncertainties were obtained by multiplying the differences in Table VII by the corresponding numbers in parentheses. The positive uncertainty is a sum of all positive terms added as though each were acting in a maximal sense without cancellation from negative contributions and similarly for the total negative uncertainty. One should bear in mind that these rather pessimistic total uncertainties are a measure of the closeness of approach of the substitutional structure to the equilibrium structure, whereas the experimental error just gives the uncertainty in the substitutional structure.

Table VII. Changes (in Å) in coordinates of the atoms of cyclopropyl chloride produced by an increase of 0.001 a.m.u. - Å² in quasi-inertial defect upon isotopic substitution.

Atom	$a^e - a$	$b^e - b$	$c^e - c$
Cl	0.0001 (6)[a]	...	0.00158 (2)
C	0.00077 (8)	...	0.00047 (2)
C	0.00019 (2)	0.00036 (2)	0.00155 (2)
H (sec)	0.00061 (8)	...	0.00020 (8)
H (cis)	0.00023 (8)	0.00022(8)	0.00030 (8)
H (trans)	0.00013 (8)	0.00024 (8)	0.00075 (8)

[a]The numbers in parentheses are the factors by which the corresponding differences were multiplied to obtain the uncertainties in Table V.

4.4 Quadrupole Analysis

Equation (2-28) for the quadrupole energy of a near symmetric top with one quadrupole nucleus can be written as

$$W_Q = aq_m + \beta q_m .$$

Transition frequencies are

$$\nu = \Delta a q_m + \Delta\beta q_m . \tag{4-11}$$

The frequency difference between hyperfine components within a given transition becomes

$$\delta\nu = (\Delta a) q_m + (\Delta\beta) q_m . \tag{4-12}$$

The constants $\delta(\Delta a)$ and $\delta(\Delta\beta)$ were computed using the observed rotational constants, and q_m and $q_m \eta$ were fit by least squares. With the a-axis most nearly representing a symmetry axis in cyclopropyl chloride, the quadrupole coupling constants are

$$\begin{aligned} \chi_{aa} &= eQq_m \\ (\chi_{bb} - \chi_{cc}) &= eQ\eta q_m \\ (\chi_{aa} + \chi_{bb} + \chi_{cc}) &= 0. \end{aligned} \tag{4-13}$$

The coupling constants (χ_s) in the principal axis system (a, b, c) must be first referred to the quadrupole tensor axis system (x, y, z) before their contribution to the bonding is discussed. This is so since the principal coupling constants are the values which are assumed in interpretations of quadrupole coupling of the molecule. In first order quadrupole effects the off diagonal matrix elements (χ_{ab} etc.) are zero and therefore dropped.

A simple rotation of axes will carry (a, b, c) into (x, y, z). With a plane of symmetry such as the a, c-plane in cyclopropyl chloride the

transformation equations are

$$\chi_{zz} = \frac{\chi_{aa} \cos\theta_z - \chi_{cc} \sin\theta_z}{\cos\theta_z - \sin\theta_z}$$

$$\chi_{xx} = \frac{\chi_{aa} \sin\theta_z - \chi_{cc} \cos\theta_z}{\sin\theta_z - \cos\theta_z} \qquad (4\text{-}14)$$

$$\chi_{yy} = \chi_{bb}.$$

The problem then becomes the evaluation of θ_z the angle between the (a, b, c) and (x, y, z) axis systems. If one assumes the z-axis of the tensor lies along the CCl bond, θ_z is computed geometrically from the structure. Otherwise, one usually assumes a cylindrical charge distribution about the CCl bond. This implies the restrictions

$$2\chi_{bb} = 2\chi_{yy} = 2\chi_{xx} = -\chi_{zz}$$

with

$$\chi_{aa} = \chi_{zz} \frac{3\cos\theta_z - 1}{2} . \qquad (4\text{-}15)$$

Table VIII gives the quadrupole coupling constants for $C_3H_5{}^{35}Cl$ for both assumptions where the standard method of differentiation was applied in the error analysis.

4.5 Discussion

Table IX lists the structural parameters of cyclopropyl chloride and a number of related compounds.

The CC bond distance in C_3H_5Cl is longer than CC distances adjacent to multiple bonds as in CH_3CCH (50) and 1,4-butadiene (51), but somewhat shorter than those found in the unstrained tetrahedral CC bonds of ethyl chloride (43) and 2-chloropropane (42). Coulson and Moffitt (15) predicted just such a shortening. In their bent bond picture the carbon

Table VIII. Quadrupole coupling constants in $C_3H_5{}^{35}Cl$.

	Principal axes	
eQq_a	= -56.64 ± 0.40 Mc	
eQq_b	= 16.80 ± 0.20 Mc	
η [a]	= - 0.2966 ± 0.0042	
χ_{bb}	= 36.72 ± 0.22 Mc	
χ_{cc}	= 19.92 ± 0.22 Mc	
	Bond axes	
	I[b]	II[c]
eQq_{zz}	-71.40 ± .51 Mc	-73.45 ± 0.44 Mc
η bond[d]	.029 ± .011	0
θ_z	21.9°	23.0 ± 0.1
I	.20	.18

[a] $\eta = (\chi_{bb} - \chi_{cc})/\chi_{aa}$

[b] Assuming θ_z = angle between CCl bond and the a-axis.

[c] Assuming cylindrical charge distribution.

[d] $\eta_{bond} = (\chi_{xx} - \chi_{yy})/\chi_{zz}$. y-axis is perpendicular to plane of symmetry.

Table IX. Comparison of structural parameters of cyclopropyl chloride with those of related molecules.

Molecule	r(CC)	r(CCl)	r(CH)	∠HCH	χ_{zz}	$\chi_{xx} - \chi_{yy}$
CH_3CH_2Cl[a]	1.520	1.788	1.090*	108.8*	-68.8	-2.4
$CH_2 = CHCl$[b,v]	1.332	1.726	1.078*	119.5	-76.9	10.0
$(CH_3)_2CHCl$[c]	1.522	1.798	1.091*	108.7*	-67.8	-1.8
CH_2CH_2CHCl[d]	1.514*	1.740	1.080*	116.2	-71.4	-2.0
$CH_2CH_2CCl_2$[e]	1.533	1.734	1.085	117.5	-76.4	-2.4
$CH_2CH_2CH_2$[f]	1.524					
$CH = CHCH_2$[g]	1.300[v] 1.515		1.070[v] 1.087	114.7		
CH_2CH_2O[h]	1.472		1.082	116.7		
CH_2CH_2S[i]	1.492		1.078	116.0		
$CH_3C \equiv CH$[j]	1.46					

[a]Reference (43). [b]Reference (44). [c]Reference (42). [d]Reference (45) [e]Reference (46). [f]Reference (47). [g]Reference (48). [h]Reference (49) [i]Ibid. [j]Reference (50). *Averages. [v]The value for parameters where the carbon atom involved has a double bond.

ring orbitals are hybridized with more p-character to give an optimum orbital angle of 104° for cyclopropane. The shorter CC bond length observed in cyclopropyl chloride plus the close agreement with their predicted HCH angle of 116°, suggests that the ring orbital angle is roughly 104°. Hence, the angle between the inter-nuclear line and the carbon orbital, the so-called strain angle, must be 1/2(104° - 60°) = 22°. The ease of electrophilic addition reactions that closely parallel those of ethylene are explained by the increased electron density located away from the ring nuclei. Emphasis must be placed on the fact that even though the internuclear distance is 1.514 Å, the distance along the orbitals is 1.552 Å which nicely conforms to the naive concept that longer bonds are weaker bonds.

Since the CCC orbitals in C_3H_5Cl have more p-character, the CH bond hybridization should be intermediate between sp^3 and sp^2. As expected, the CH bond length is shorter than the average CH in sp^3 hybrids (1.09 Å) yet is greater than the vinyl CH distances in cyclopropene (48) and vinyl chloride (44). Like the other three-membered rings in Table IX, the HCH angle lies between the "normal" tetrahedral and trigonal angles of 109° and 120°.

While the plane formed by the carbon ring of cyclopropane is a plane of symmetry, the methylene groups of C_3H_5Cl are no longer mirror images through the plane of the ring. A glance at Figure 2 and Table V illustrates that the cis hydrogens are pinched in toward one another and directed at the chlorine atom.

Contrary to the other parameters, the CCl distance in cyclopropyl chloride does not appear to be situated between sp^2 and sp^3 bonding. In fact, the r(CCl) approaches the bond distance found in vinyl chloride.

An empirical linear relationship existing between bond length and the chlorine quadrupole coupling constant in saturated mono-chloro hydrocarbons has recently been plotted (42). However, the point for cyclopropyl chloride does not fall on that line, either because χ_{zz} is too small, or because the CCl bond distance is too short. It can be argued that a bent CCl bond would achieve the same shortening. Yet, in the study of 1,1-dichlorocyclopropane (46) where off diagonal elements of the quadrupole coupling constant matrix are available, the maximum electron density is shown to lie along the internuclear direction, thereby ruling out a bent CCl bond. A second look at equation (2-29)

$$I = (1 - s^2 + d^2 + II) - \chi_{zz}/eQq_{atom})$$

discloses that increased π bonding, II, and decreased ionic character, I, oppose one another in evaluation of the quadrupole coupling constant while both effects tend to shorten bond lengths. The most straightforward interpretation involves less ionic character and more π bonding due to the p_x and p_y lone pair chlorine orbital electrons. The same situation is found in vinyl chloride where a difference of 10 Mc/sec in $\chi_{xx} - \chi_{yy}$ indicates the presence of a considerable π bonding contribution from the p-orbital of chlorine perpendicular to the plane of symmetry. Since $\chi_{xx} - \chi_{yy}$ for cyclopropyl chloride is only -2.4 Mc/sec, both p_x and p_y contribute about equally to the bonding.

REFERENCES

1. Baeyer, A., Ber. 18, 2269 (1885).

2. (a) Sachse, H., N. Physic. Chem. 10, 203 (1892).

   (b) Mohr, E., J. Prakt. Chem. 103, 316 (1922).

3. Ingold, C. K., J. Chem. Soc. 119, 306 (1921).

4. Ruzicka, L., Boekenoogen and Edelmann, Helv. Chim. Acta. 16, 487 (1933).

5. Rogers, M. T. and J. D. Roberts, J. Am. Chem. Soc. 68, 843 (1946).

6. Hawthorne, M. T., J. Org. Chem. 21, 1523 (1956).

7. Perold, G. W., J. S. African Chem. Inst. 6, 22 (1953); 8, 1 (1955); 10, 11 (1957); Chem Absts. 48, 4314c (1954); 50, 6326d (1956); 52, 10741 (1958).

8. Goodman, A. L. and R. H. Eastman, J. Am. Chem. Soc. 86, 908 (1964).

9. Tuchs, R. and J. J. Bloomfield, J. Am. Chem. Soc. 81, 3158 (1959).

10. Cannon, G. W., A. A. Santilli and P. S. Shenian, J. Am. Chem. Soc. 81, 4264 (1959).

11. (a) Tractenberg, E. N. and G. Odian, Chemistry and Industry 490 (1958).

    (b) Tuchs, R., C. A. Kaplan, J. J. Bloomfield, and L. F. Hatch, J. Org. Chem. 27, 733 (1962).

12. Duffey, G. H., J. Chem. Phys. 14, 342 (1946).

13. Walsh, A. D., Trans. Far. Soc. 45, 179 (1949).

14. Peters, D., Tetrahedron 19(10), 1539 (1963).

15. Coulson, C. A. and W. E. Moffitt, Phil. Mag. 40, 1 (1949).

16. O'Gorman, J. M. and V. Schomaker, J. Am. Chem. Soc. 68, 1138 (1946).

17. Friend, J. P., and B. P. Dailey, J. Chem. Phys. 29, 577 (1958).

18. Coles, D. K. and W. E. Good, Phys. Rev., 70, 979L (1946).

19. Dakin, T. W., W. E. Good, and D. K. Coles, Phys. Rev. 70, 560 (1946).

20. Townes, C. H. and B. P. Dailey, J. Chem. Phys. 17, 782 (1949).

21. Kraitchman, J., Am. J. Phys. 21, 17 (1953).

22. Wang, S. C., Phys. Rev. 34, 243 (1929).

23. Schwendeman, R. H., J. Chem. Phys. 27, 986 (1957).

24. Ray, B. S., Zeits., f. Physik 78, 74 (1932).

25. King, G. W., R. M. Hainer, and P. C. Cross, J. Chem. Phys. 11, 27 (1943).

26. Townes, C. H. and A. L. Schawlow, Microwave Spectroscopy, McGraw-Hill, New York, 1955.

27. Goldstein, H., Classical Mechanics, Reading, Massachusetts, Addison-Wesley Publishing Company, Inc., 1950. (Chapter V).

28. Sinnott, K. M., J. Chem. Phys. 34, 851 (1961).

29. Gordy, W., W. V. Smith, and R. T. Trambarulo, Microwave Spectroscopy, John Wiley and Sons, New York, 1953.

30. Dailey, B. P. and C. H. Townes, J. Chem. Phys. 23, 118 (1955).

31. Dailey, B. P., J. Chem. Phys. 33, 1641 (1960).

32. Jacobs, G. D., Thesis, Michigan State University, (1961).

33. Tobiason, F. L., Thesis, Michigan State University, (1963).

34. Hendrick, L. C., Rev. Sci. Instr. 20, 781 (1949).

35. Hughes, R. H. and E. B. Wilson, Jr., Phys. Rev. 71, 562 (1947).

36. Todd, J. E., M. A. Whitehead, and K. E. Weber, J. Chem. Phys. 39, 404 (1963).

37. Hart, H. and R. A. Cipriani, J. Am. Chem. Soc. 84, 3697 (1962).

38. Roberts, J. D., J. Am. Chem. Soc. 67, 1281 (1945).

39. Schwendeman, R. H., J. Mol. Spec. 6, 301 (1961).

40. Costain, C. C., J. Chem. Phys. 29, 864 (1958).

41. Laurie, V. W., Symposium on Molecular Structure and Spectroscopy, Ohio State University, June, 1963.

42. Tobiason, F. L. and R. H. Schwendeman, J. Chem. Phys. 40, 1014 (1964).

43. Schwendeman, R. H. and G. D. Jacobs, J. Chem. Phys. 36, 1245 (1962).

44. Kivelson, D., E. B. Wilson, Jr., and D. R. Lide, Jr., J. Chem. Phys. 32, 205 (1960).

45. Schwendeman, R. H., G. D. Jacobs, and T. M. Krigas, J. Chem. Phys. 40, 1022 (1964).

46. Flygare, W. H. A. Narath and W. D. Gwinn, J. Chem. Phys. 36, 200 (1962).

47. Baker, A. W. and R. C. Lord, J. Chem. Phys. 23, 1636 (1955).

48. Kasii, P. H. and R. J. Myers, J. Chem. Phys. 30, 512 (1959).

49. Cunningham, G. L., A. W. Boyd, R. J. Myers, W. D. Gwinn, and W. I. Le Van, J. Chem. Phys. 19, 676 (1951).

50. Trambarulo, R. and W. Gordy, J. Chem. Phys. 18, 1613 (1950).

51. Schomaker, V. and L. Pauling, J. Am. Chem. Soc. 61, 1769 (1939).